Journal of Materials Science and Chemical Engineering, 2026, 14(8), 140-167
https://www.scirp.org/journal/msce
ISSN Online: 2327-6053
ISSN Print: 2327-6045

Theoretical Analysis of LMTD, Thermal Effectiveness, and Thermal Efficiency Methods Applied to Chevron Plate Heat Exchangers (CPHEs)

João Vitor Santana, Élcio Nogueira

Departamento of Mecânica e Energia (DME), Universidade do Estado do Rio de Janeiro (FAT/UERJ), Resende, Brazil
Email: elcionogueira@hotmail.com

How to cite this paper: Santana, J.V. and Nogueira, É. (2026) Theoretical Analysis of LMTD, Thermal Effectiveness, and Thermal Efficiency Methods Applied to Chevron Plate Heat Exchangers (CPHEs). *Journal of Materials Science and Chemical Engineering*, **14**, 140-167.
https://doi.org/10.4236/msce.2026.148008

Received: April 17, 2026
Accepted: August 25, 2026
Published: August 28, 2026

Abstract

This article presents a practical and low-cost procedure for the preliminary prediction of the performance of chevron plate heat exchangers (CPHEs), also pointing to broader design and research topics—such as the relationship between pressure drop and heat transfer, geometric optimization, irreversibility, and advanced working fluids—that can be explored beyond the base case. Some solutions and discussions presented in the article are the result of challenge proposed to students completing a Mechanical Engineering course, in subjects related to Energy Efficiency. The article presents theoretical results for four chevron plate heat exchangers (CPHEs), with the objective of analysis, theoretical-experimental comparisons, and discussions. Experimental and numerical results from published literature are used as a reference. The authors of the reference work present theoretical results applying an analytical procedure, called the bisection method, to the four different types of compact heat exchangers. In the present article, the methods used for theoretical reproduction are the logarithmic mean temperature difference (LMTD) method, the thermal effectiveness (ε-NTU) method, and the efficiency thermal method, with emphasis on the latter. A more detailed theoretical analysis is applied to the first of the four heat exchangers, with graphical results for the outlet temperatures of the working fluids. In this first approach, theoretical-experimental comparisons show deviations ranging from 1% to 4%, with the heat exchanger area defined through the reference work. Graphical results for thermal effectiveness and heat transfer rate are obtained from data taken from the reference work, using temperature and mass flow rate ranges, and applying the thermal efficiency method. Additionally, tabulated values are used to present results obtained for the last 3 heat exchangers analyzed. In these cases, theoretical-experimental comparisons for outlet temperatures, with real heat transfer areas calculated from experimental data, range from 0.00% to 1.01%.

Keywords

Chevron Plate Heat Exchangers (CPHEs), Bisection Method, LMTD Method, Thermal Effectiveness Method (ε-NTU), Thermal Efficiency Method

1. Introduction

This work presents a practical and low-cost procedure for the preliminary prediction of the performance of chevron plate heat exchangers (CPHEs), aiming to reproduce, expand, and critically discuss the theoretical and experimental results reported by Bhattad *et al.* [1] for the chevron plate heat exchangers (CPHEs). To reproduce the outlet temperatures and evaluate the performance of the CPHE, the work adopts the bisection method coupled with classical approaches to heat exchanger analysis: the logarithmic mean temperature difference (LMTD) method, the thermal effectiveness method (ε-NTU), and the thermal efficiency method (based on the fin analogy and the concepts of the second law of thermodynamics).

In this introduction, we include references that contextualize relevant current literature on CPHEs, including empirical correlations, CFD-based thermohydraulic analyses, studies on tilt angle optimization, effects of poor flow distribution, and performance improvement with nanofluids.

The researchers in the article used as a reference in this work, Atul Bhattad *et al.* state that the design of heat exchangers involves a complex interaction of factors. They report that these factors include cost, maintenance, material selection, pressure drop, flow configuration, and heat transfer. They emphasize that the complexity of the designs generally involves empirical relationships for performance evaluation. They highlight the need for tests to obtain outlet temperatures, inlet parameters, and the physical characteristics of the working fluids. The article presents a reliable procedure for estimating fluid outlet temperatures. The procedure is based on basic equations for the heat transfer rate and the logarithmic mean temperature difference (LMTD). Validation of the theoretical predictions is obtained through comparisons with experimental data. The authors highlight the adaptability of the bisection method and propose its application to other types of heat exchangers. Regarding the comparisons made, they indicate a relative error of 1.8% to 2.6% for the cold fluid temperatures and a relative error of 2.4% to 3.5% for the hot fluid outlet temperatures. They add that the proposed method allows for a preliminary assessment of the heat exchanger's performance before carrying out expensive and time-consuming tests.

Élcio Nogueira [2] publishes a book on theories and applications related to heat exchangers. The theories developed relate to thermal irreversibilities and viscous irreversibilities. This theory encompasses concepts generally applied in heat exchangers but innovates by introducing and applying the Thermal Efficiency Method. The Thermal Efficiency Method, which uses the concept known as the "Fin Analogy", is very similar to the Effectiveness Method (ε-NTU), but introduces a new concept when dealing with thermal irreversibilities. A heat exchanger with optimal thermal performance exhibits high thermal irreversibility, characterized by its thermal effectiveness. Thermal efficiency, in turn, represents the potential associated with the physical configuration of the exchanger that would allow for maximum heat exchange. The potential associated with thermal efficiency, however, does not represent the actual rate of heat transfer between the fluids, which is represented by thermal effectiveness, the ratio between the heat transfer rate obtained through the current configuration under analysis and the maximum theoretically possible heat transfer rate. The Thermal Efficiency Method innovates by considering the heat exchange between fluids and has the characteristic of being simple to implement, without the need for nomograms or complex equations, regardless of the heat exchanger configuration, and thermal effectiveness can be derived using it. In the aforementioned book, two chapters deal specifically with chevron plate heat exchangers: Chapter 5: "Entropy generation rate in a chevron plate heat exchanger"; Chapter 6: "Dimensionless analysis of a chevron plate heat exchanger using the second law of thermodynamics".

Yi Zhao *et al.* [3] performed a numerical analysis related to the effect of the chevron plate angle on the thermo-fluid dynamic characteristics of heat exchangers. They analyzed heat exchangers with a plate diameter of 215 mm and chevron angles of 30˚, 45˚, 60˚, and 75˚. They presented performance results for heat transfer and friction. They observed that the Nusselt number and the friction factor on the shell side increase with increasing chevron angle. They highlighted that, for the same inlet flow rate, the pressure profile on the shell side changes significantly with the chevron angle. They found that the best performance occurs with a chevron angle of 45˚, applicable to both the shell and plate sides.

Adarsh Varma P. *et al.* [4] utilize heat exchanger systems and nanofluids with the aim of improving thermal efficiency. They highlight that nanofluids exhibit better thermal conductivity in heat exchangers. The article reviews, analyzes, and discusses research from various groups on the use of nanofluids. The main conclusion of the work highlights and suggests the use of nanofluids in heat exchangers, since their use enables better thermal performance.

Olga Arsenyeva *et al.* [5] states that plate heat exchangers (CPHEs) are modern and efficient, with the capacity to increase heat recovery and energy efficiency. They present a review and analysis of the main developments and modifications in the construction of plate heat exchangers, which influence thermal and hydraulic performance. They highlight that modern exchangers have plates with inclined corrugations, which create robust and rigid construction with multiple points of contact between the plates. They emphasize that the main corrugations are related to the angles of inclination of the corrugation in relation to the direction of the main flow and the aspect ratio of the corrugation, and that the optimization of these aspects has improved the performance of plate heat exchangers. They discuss possible lines of future research related to the development of new corrugation shapes and optimization methods.

Zhang J. *et al.* [6] experimentally and numerically studied the heat transfer and flow resistance characteristics of a plate heat exchanger with corrugated slots in multiple chevrons. The numerical results showed good agreement with experimental values. The shear stress transport model k ~ w is recommended for simulating the plate heat exchanger. They demonstrated that high-temperature regions are distributed on the left side of the heat exchanger, while low-temperature regions are distributed on the right side, resulting in rotational flow. This effect provides better heat transfer and greater pressure drop.

Jeong Gyun Ham *et al.* [7] state that poor flow distribution in plate heat exchangers impairs the intended optimal performance and that the impact on performance depends on the number of channels in the plate heat exchanger. They use computational fluid dynamics (CFD) to identify the effects of poor flow distribution and the appropriate location for the installation of the measuring device. They demonstrated that channels located at the end of the manifold exhibit excessive flow, while channels near the tube exhibit relatively low flow. They found that jet flow occurs when the fluid flows from the channel to the outlet manifold, resulting in non-uniform velocity and temperature distribution. However, they demonstrate that, due to turbulent flow, the mass flow and temperature distribution in the tube becomes uniform.

Sohn S. *et al.* [8] conducted a study on the effect of flow path on heat transfer and pressure performance in a plate heat exchanger. They used computational fluid dynamics (CFD) and developed a numerical model to evaluate the heat transfer and flow characteristics. As a result of the study, it was found that curved flow performs better than straight flow in terms of heat transfer and pressure loss. It was observed that the performance becomes more evident with increasing flow rate.

García-Castillo J.L. *et al.* [9] present a new design approach for framed plate heat exchangers for single-flow and multi-channel units, and corrugations. They highlight that the corrugation angle becomes a degree of freedom and can be modified to meet a specific thermal load. They worked on the design of a two-flow heat exchanger and found that the best configuration is obtained for a corrugation angle of 46˚ and 166 thermal plates. They demonstrated that five single-phase heat exchangers can be replaced by a single multi-channel unit, with an equivalent 55% reduction in final cost.

Ali Sadeghianjahromi *et al.* [10] experimentally and numerically studied the effect of the angle of inclination on the Thermofluids dynamic characteristics of brazed plate heat exchangers (BPHEs). They simulated the effects of brazing joints and the distribution of inlet/outlet ports, which are generally neglected in existing literature. Four types of BPHEs were considered, with different angles of inclination: 35˚; 50˚; 65˚; 35˚/65˚. The results demonstrated that increasing the angle of inclination leads to an increase in the Nusselt number and the friction factor. The flow study illustrates that increasing the angle of inclination leads to a change in the flow pattern, which causes an increase in the heat transfer rate and pressure drop. They developed correlations for the Nusselt number and the friction factor with average deviations of 9%.

Élcio Nogueira [11] applies different methods for the theoretical determination of the thermal and hydraulic performance of a plate heat exchanger. The work analyzes the impact of the chevron inclination angle through a theoretical model applied to a sunflower vegetable oil cooler. Comparisons are made with experimental results from the literature for inclination angles of 30˚, 45˚, and 60˚. In addition to the inclination angle, two other parameters, the mass flow rate of the cold fluid and the number of plates, are considered crucial for the analysis of the results. The results point to the need to improve the methods applied to plate heat exchangers with gaskets, considering the influence of the inclination angle, since there are significant differences between the results obtained and analyzed.

Élcio Nogueira [12] addresses the thermo-hydraulic performance of a plate heat exchanger with gaskets, used for cooling vegetable oils, with a mixture of water and ethylene glycol (50%) and volumetric fractions of non-spherical nanoparticles as refrigerant. The heat exchanger has 75 plates with an inclination angle of 30º. The non-spherical nanoparticles used in the analysis are of the platelet, cylindrical, and block-shaped type. The results obtained allow us to conclude that it is possible to work with low relative flow rates using non-spherical nanoparticles, with emphasis on platelet-shaped nanoparticles. The entropy generation analysis shows that very high refrigerant flow rates dissipate a large part of the energy in viscous form and do not contribute to oil cooling, with a consequent increase in the operating costs of the heat exchanger.

Tiari R. Rezende *et al.* [13] investigate the use of nanofluids in plate heat exchangers through 3D CFD simulations. For the analysis, the corrugation angles of the plates were varied between 0˚ and 60˚. The model validation was performed using experimental data obtained for the heat transfer coefficients. The results demonstrate that the use of nanofluids, in high concentrations, improves the performance of the thermal parameters and that angles between 30˚ and 60˚ reduce the pressure drop and reflux regions. The authors report that, in general, the applied method can be advantageously used to improve the design of plate heat exchangers.

Sanjem Kumar Gupta *et al.* [14] present an article that provides an overview of the use of nanofluids in a plate heat exchanger. They highlight that heat exchangers are components used in various domestic and industrial applications. They consider that economic aspects and improved thermal performance are the main challenges. They state that the use of nanofluids is one of the best options to increase the heat transfer rate.

Dutta OY and Rao BN [15] present empirical relationships for chevron-type plate heat exchangers and, through experimental tests, demonstrate their validity.

They examine the pressure drop (ΔP), the overall heat transfer coefficient, and the thermal effectiveness. The quantities are estimated as a function of the plate material properties, the working fluid, the number of plates (Nt), and the chevron angle (β). They find that increasing the number of plates, without altering other dimensions, avoids the need for a new design. They apply Taguchi's method to reduce the number of experiments, defining parameter levels and comparing the test data with the theoretically estimated values.

Élcio Nogueira [16] uses the second law of thermodynamics to determine the theoretical optimum thermal performance of a chevron plate heat exchanger. In his analysis, he considers the variation in refrigerant flow rate, the variation in the total number of plates in the heat exchanger, the effect of the chevron tilt angle, and the influence of the fouling factor. He presents graphical results for thermal efficiency, thermal irreversibility, thermal effectiveness, heat transfer rate, and outlet temperatures of water and oil. He demonstrates that a defined number of plates allows for the best theoretical thermal performance of the heat exchanger and that the theoretical optimum number depends on all the listed factors.

2. Methodology

This work reproduces the Bisection Method (LMTD), used for comparison with experimental results published through reference. For comparison and analysis purposes, using experimental data, the theories associated with the Logarithmic Mean Temperature Difference Method (LMTD), the Effectiveness Method (ε-NUT), and the Thermal Efficiency Method are applied. Results obtained are presented through tables and graphs.

The methods implemented in this work, specifically, are: Logarithmic Mean Temperature Difference (LMTD), through the computational implementation of the bisection method, for comparison with the same method used in the original work, and which is defined by Equation (7) below, with precision probably different from the original work, since this data is not accessible in the work reference; Number of Thermal Units or Effectiveness Method (ε-NTU); Thermal Efficiency Method.

The authors of reference work use data from industrial heat exchangers, imposing input conditions for physical parameters associated with the heat exchangers and the working fluids, to determine the outlet temperatures of four different types of CPHE.

Figure 1 shows the plates of the chevron plate heat exchanger, with details related to the plate angle.

2.1. Formulation of the Theoretical Solution Procedures Adopted

Energy balance between fluids is represented by Equation (1) below:

$$\dot{m}_h C_{ph}\left(T_{hi} - T_{ho}\right) = \dot{m}_c C_{pc}\left(T_{co} - T_{ci}\right) \tag{1}$$

with,

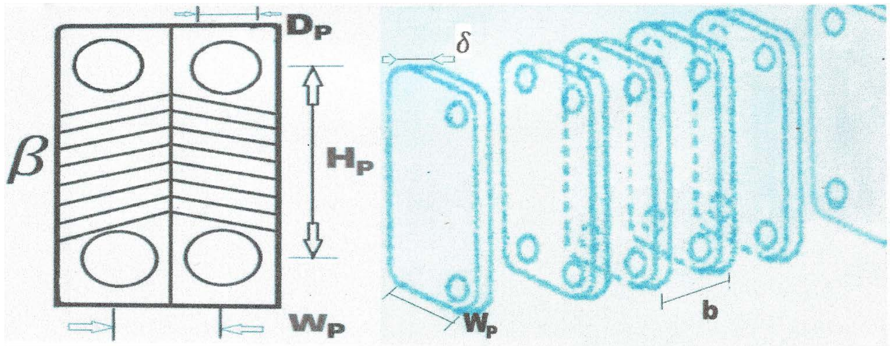

Figure 1. Representation of a Chevron Plate Heat Exchanger (CPHE) [1].

$$0.1896\frac{\text{kg}}{\text{s}} \le \dot{m}_h \le 0.6139\frac{\text{kg}}{\text{s}};\ 0.1890\frac{\text{kg}}{\text{s}} \le \dot{m}_c \le 0.6147\frac{\text{kg}}{\text{s}} \tag{1.1}$$

$$59.15^\circ\text{C} \le T_{hi} \le 61.89^\circ\text{C};\ 28.46^\circ\text{C} \le T_{ci} \le 40.08^\circ\text{C} \tag{1.2}$$

$$4066.7\frac{\text{J}}{\text{kg}\cdot\text{K}} \le C_p \le 4066\frac{\text{J}}{\text{kg}\cdot\text{K}};\ 4983.39\frac{\text{W}}{\text{m}^2\cdot\text{K}} \le U_o \le 9608.88\frac{\text{W}}{\text{m}^2\cdot\text{K}} \tag{1.3}$$

where,

$\dot{m}_h$ and $\dot{m}_c$ are the mass flow rates of the hot and cold fluids, respectively.

C_{ph} and C_{pc} are the specific heats of the hot and cold fluids, respectively.

T_{hi} and T_{ho} are the inlet and outlet temperatures of the hot fluid, respectively.

T_{ci} and T_{co} are the inlet and outlet temperatures of the cold fluid, respectively.

The input variables required to determine the thermal performance of the heat exchanger, using the procedures under analysis, are: T_{hi}, T_{ci}, $\dot{m}_h$, $\dot{m}_c$, C_{ph}, C_{pc}. A_{transf} e U_o.

A_{transf} is the heat exchange area associated with the heat exchanger, U_o is the overall heat transfer coefficient, both defined as a priori.

The physical quantities used in this work, in all simulations performed, are represented by Equations and Tables obtained from reference [1], including the ranges of values for the overall heat transfer coefficients.

2.1.1. Solution Using the Bisection Method (LMTD)

The logarithmic mean temperature difference (LMTD) method is expressed by the relationship between the inlet and outlet temperatures of the cold and hot fluids used in the heat exchanger by Equation (2) below.

$$T_{ho} = T_{hi} - \left(U_O A_{Transf}\right) / \left(\dot{m}_h C_{ph}\right) \Delta T_{lm} \tag{2}$$

ΔT_{lm} is called the logarithmic mean temperature difference, obtained through Equation (3).

$$\Delta T_{lm} = \left(\Delta T_1 - \Delta T_2\right) / \left(l_n\left(\Delta T_1 / \Delta T_2\right)\right) \tag{3}$$

where,

$$\Delta T_1 = T_{hi} - T_{co} \text{ and } \Delta T_2 = T_{ho} - T_{ci} \tag{4}$$

T_{ho} is obtained as a function of T_{co} through Equation (5), after final determination of T_{co}.

$$T_{ho} = T_{hi} - (\dot{m}_c C_{pc})/(\dot{m}_h C_{ph})(T_{co} - T_{ci}) \quad (5)$$

Substituting Equation (5) into Equation (2), we have:

$$T_{hi} - (\dot{m}_c C_{pc})/(\dot{m}_h C_{ph})(T_{co} - T_{ci}) = T_{hi} - (U_O A_{Transf})/(\dot{m}_h C_{ph})\Delta T_{lm} \quad (6)$$

Therefore, we have:

$$f(T_{co}) = (U_O A_{Transf})/(\dot{m}_h C_{ph})\Delta T_{lm} - (\dot{m}_c C_{pc})/(\dot{m}_h C_{ph})(T_{co} - T_{ci}) \quad (7)$$

where $f(T_{co}) = 0$.

$f(T_{co}) = 0$ is a non-linear equation, where the unknown variable is T_{co}.

$$\dot{Q} = U_o A_{tranf} \Delta T_{lm} \quad (8)$$

One of the approaches used to obtain T_{co} is the bisection method, which consists of dividing the interval between two initially arbitrary values. T_a and T_b for T_{co}, through the following iterative procedure:

$$1. \quad f(T_a) < 0 \quad \text{e} \quad f(T_b) > 0 \quad \text{find} \quad T_m = \frac{T_a + T_b}{2} \quad (9)$$

$$2. \text{ If } \quad f(T_a) * f(T_b) < 0 \rightarrow T_a = T_m \rightarrow T_m = \frac{T_a + T_b}{2} \quad (10)$$

$$3. \text{ If } \quad f(T_a) * f(T_b) > 0 \rightarrow T_b = T_m \rightarrow T_m = \frac{T_a + T_b}{2} \quad (11)$$

Repeat steps (2, 3) above until $|f(T_m)| < \varepsilon_0$. With ε_0 a precision defined a priori.

2.1.2. Solution Using the Thermal Effectiveness Method (ε-NUT)

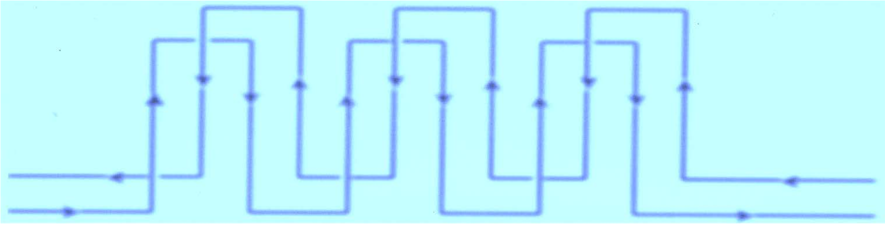

Figure 2. Counterflow configuration for working fluids in CPHE [1].

Figure 2 schematically presents the counterflow configuration for the CPHE heat exchangers under analysis.

The thermal effectiveness ε_T is obtained through the parameters already defined for the heat exchanger, namely ε-NUT:

$$\varepsilon_T = \frac{1 - e^{-NTU(1-c^*)}}{1 - c^* e^{-NTU(1-c^*)}} \quad \text{for counter flow} \quad (12)$$

where,

$$NTU = \left(U_O A_{Transf}\right) / C_{min} \tag{13}$$

NTU is the number of thermal units associated with the heat exchanger.

$C^* = C_{min}/C_{max}$ is the relationship between the minimum and maximum thermal capacities of the heat exchanger, where: $C_h = \dot{m}_h C_{ph}$ and $C_c = \dot{m}_c C_{pc}$. C_{min} is the lowest of the thermal capacities among fluids.

The outlet temperature of the hot fluid is obtained using Equation (13), below:

$$T_{ho} = T_{hi} - \varepsilon_T \left(T_{hi} - T_{ci}\right) \tag{14}$$

From Equations (5) and (14), we have:

$$\varepsilon_T C_{min} (T_{hi} - T_{ci}) = \dot{m}_c C_{pc} \left(T_{co} - T_{ci}\right) \tag{15}$$

The value of the cold fluid outlet temperature, T_{co}, is obtained by Equation (15), below:

$$T_{co} = T_{ci} + \varepsilon_T \left(T_{hi} - T_{ci}\right) \tag{16}$$

$$\dot{Q} = \varepsilon_T C_{min} \left(T_{hi} - T_{ci}\right) \tag{17}$$

$\dot{Q}$ is heat transfer rate.

2.1.3. Solution Using the Thermal Efficiency Method

The thermal efficiency η_T is obtained through the parameters already defined for the heat exchanger, namely:

$$\eta_T = \tanh\left(Fa\right) / Fa \tag{18}$$

The number of fin analogy (Fa) [17] is obtained through the following expression for counterflow:

$$Fa = NTU\left(1 - C^*\right) / 2 \quad \text{for counterflow} \tag{19}$$

with,

$$NTU = \left(U_O A_{Transf}\right) / C_{min} \tag{20}$$

$C^* = C_{min}/C_{max}$ is the relationship between the minimum and maximum thermal capacities of the heat exchanger, where: $C_h = \dot{m}_h C_{ph}$ e $C_c = \dot{m}_c C_{pc}$. C_{min} is the lowest of the thermal capacities among fluids.

The value of the cold fluid outlet temperature, T_{co}, is obtained through thermal efficiency by Equation (21) [2].

$$T_{co} = T_{ci} + 1 \Big/ \left(1 / \left(\eta_T NTU\right) + \left(1 + c^*\right) / 2 \right) * C_{min} \Big/ \left(\dot{m}_c C_{pc}\right) * \left(T_{hi} - T_{ci}\right) \tag{21}$$

$$T_{ho} = T_{hi} - 1 \Big/ \left(1 / \left(\eta_T NTU\right) + \left(1 + c^*\right) / 2 \right) * C_{min} \Big/ \left(\dot{m}_c C_{pc}\right) * \left(T_{hi} - T_{ci}\right) \tag{22}$$

The rate of heat transfer, $\dot{Q}$, is obtained through the equation below.

$$\dot{Q} = 1 \Big/ \left(1 / \left(\eta_T NTU\right) + \left(1 + c^*\right) / 2 \right) * C_{min} * \left(T_{hi} - T_{ci}\right) \tag{23}$$

Thermal effectiveness can be obtained through thermal efficiency, using the equation below:

$$\varepsilon_T = 1\Big/\Big(1/(\eta_T NTU) + \big(1+c^*\big)/2\Big) \tag{24}$$

3. Results and Discussion

The reference theoretical-experimental analysis [1] uses 4 different types of CPHE, with distinct characteristics.

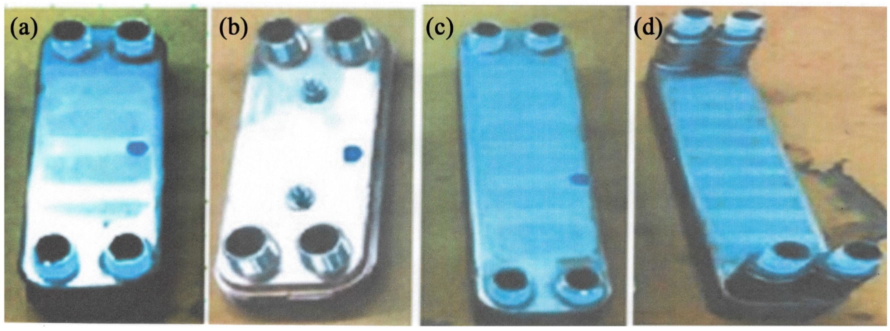

Figure 3. Compact chevron plate heat exchangers under analysis [1].

Figures 3(a)-(d) show the four distinct types of CPHE under analysis. The heat exchangers Figures 3(a)-(d) represented above will be referred to as CPHE-1, CPHE-2, CPHE-3 and CPHE-4, respectively.

Analysis and Discussion of the Theoretical Results Obtained for CPHE-1

The CPHE-1 (3A) is the reference heat exchanger, whose detailed analysis and discussion is carried out through the graphical results presented in this section.

Figure 4. Chevron Plate Heat Exchanger—CPHE-1 [1].

The CPHE-1 heat exchanger, with the dimensions specified by the reference work, is shown in Figure 4.

The authors of the reference work applied the bisection method through a theoretical-experimental approach. They obtained theoretical-experimental results for cold and hot fluid flow rates, inlet temperatures for cold and hot fluids, and outlet temperatures for cold and hot fluids. They include numerical results and convergence analysis through the bisection method, and graphical results for logarithmic mean temperature difference, heat transfer rate, overall heat transfer coefficient and thermal effectiveness.

This section will present graphical results, obtained through the application of the Bisection Method (LMTD), Thermal Effectiveness (ε-NUT) and Thermal Efficiency, for comparison with experimental results and the bisection method presented in reference work. The experimental data for flow rates, fluid temperatures and physical properties are obtained from the article of reference.

Theoretical-experimental comparisons for outlet temperatures of hot, Figure 5, and cold fluids, Figure 6, demonstrate that the deviations obtained through the

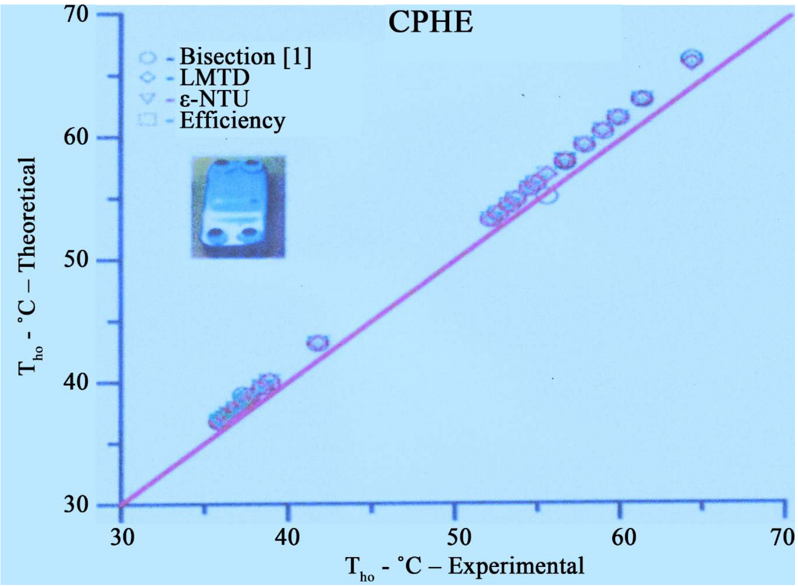

Figure 5. Theoretical-experimental comparison for T_{ho}.

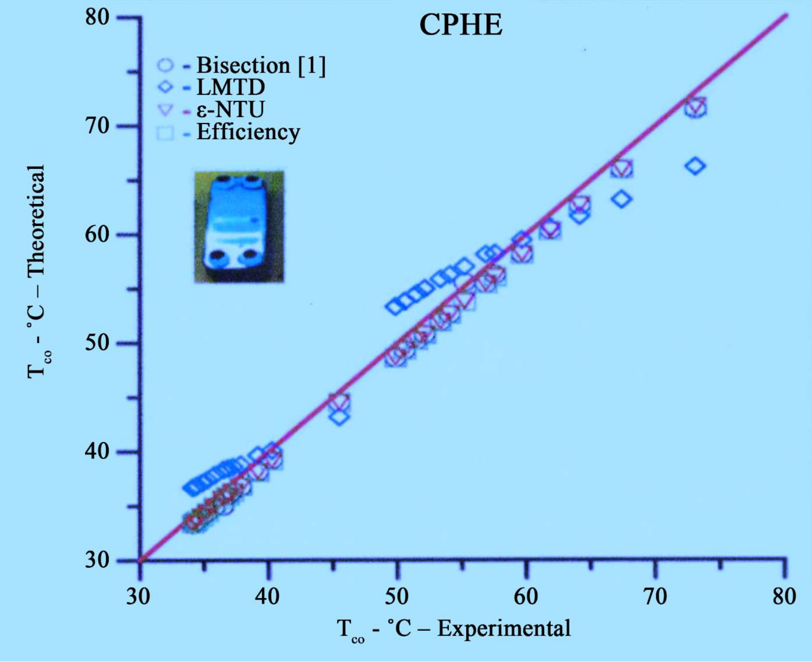

Figure 6. Theoretical-experimental comparison for T_{co}.

methods under analysis are not significant in qualitative terms.

There is a slight discrepancy between the results obtained through the LMTD Method for the outlet temperatures of the cold fluid. However, the discrepancies mentioned are not very relevant, as demonstrated by the results in Figure 7 and Figure 8.

Numerical results for quantitative comparison between theoretical and experimental results for the outlet temperatures of the hot fluid (Figure 7) and cold fluid (Figure 8) are represented below. The percentage errors obtained for the hot fluid outlet temperature show results concentrated between 2.2% and 3.6%, with a single outlier for the bisection method, with a value close to 4.4%.

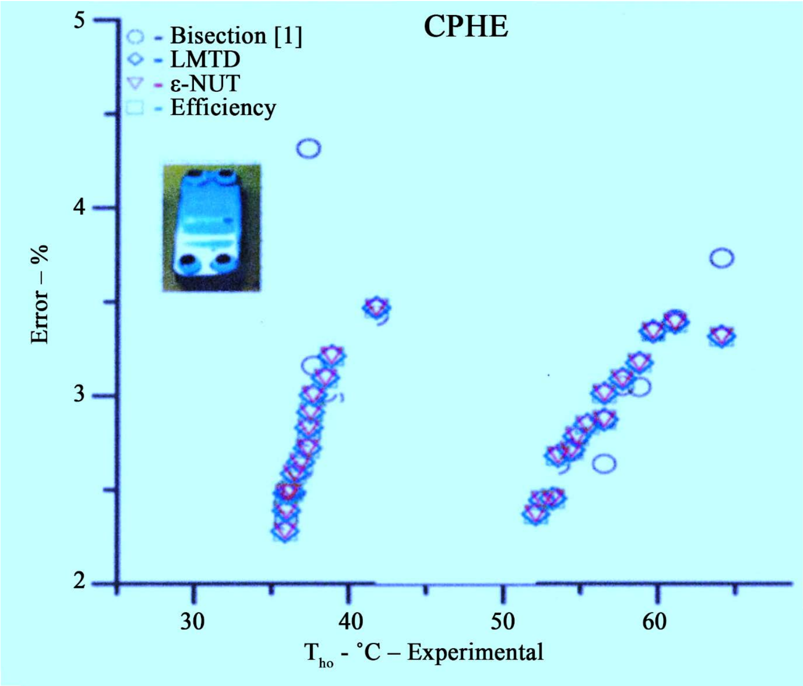

Figure 7. Percentage error for T_{ho} versus hot fluid outlet temperature.

The results obtained for comparisons between cold fluid outlet temperatures, Figure 8, show lower values than those observed for the hot fluid outlet temperature. The results vary between 1.6% and 2.8%. The differences identified between the applied methods do not present significant numerical relevance, indicating that all methods under analysis are adequately applied to the CPHE-1 heat exchanger.

Identical results are verifiable when using the hot fluid flow rate as the analysis variable, Figure 9 and Figure 10. The data presented for fluid outlets show that there are two distinct blocks for inlet temperatures, which is not very evident when using the data from reference work.

To advance in the theoretical analysis of the heat exchanger, for greater clarity in the presents experimental results obtained for the overall heat transfer coefficient as a function of the flow rate associated with the hot fluid. The estimated values, highlighted in red, are the result of interpolation between experimental results.

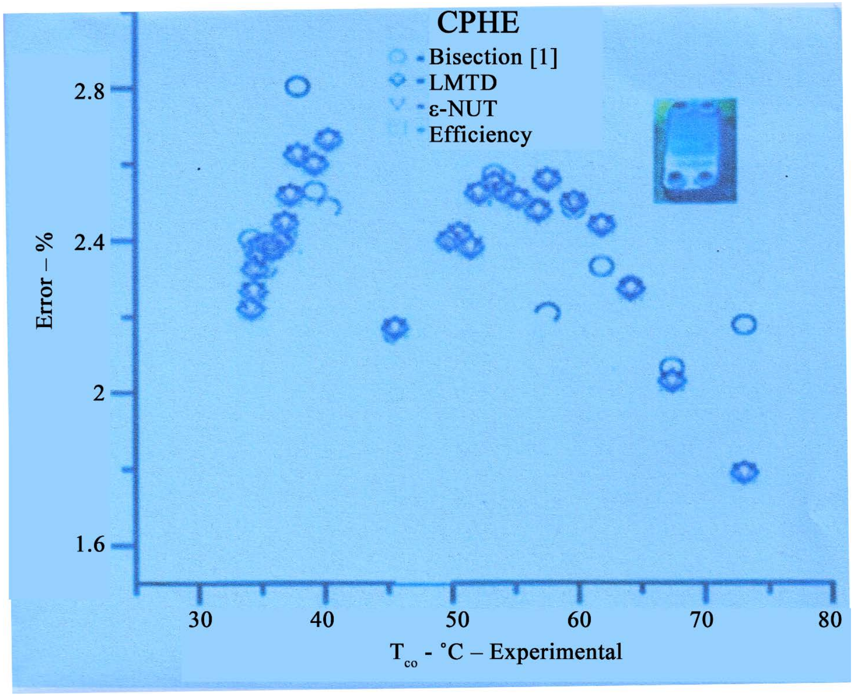

Figure 8. Percentage error for T_{co} versus cold fluid outlet temperature.

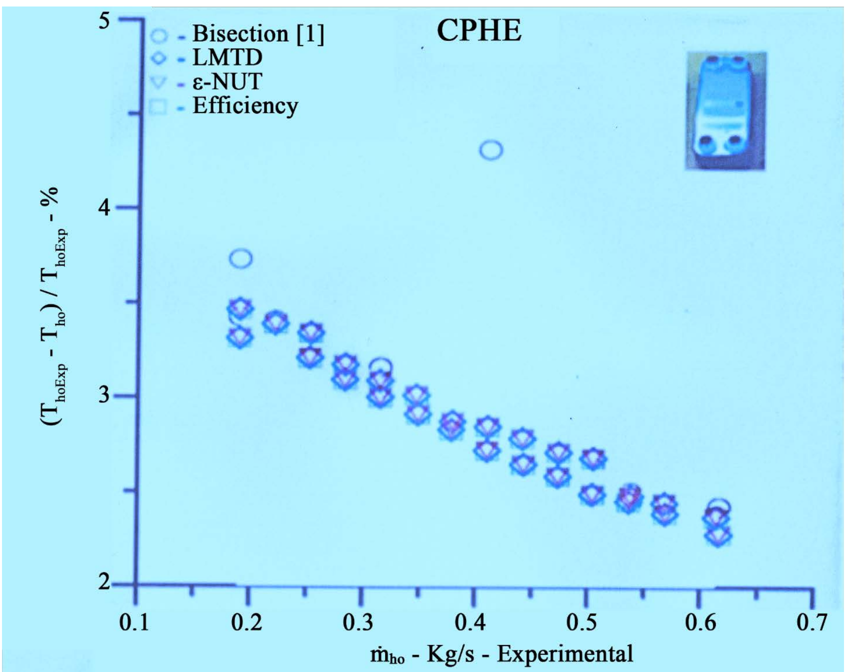

Figure 9. Percentage error for hot fluid outlet temperature T_{ho}.

The results presented demonstrate consistency in the implemented theoretical models, as the deviations obtained are validated across all flow rate and inlet temperature ranges for CPHE-1.

The results highlighted in red, in **Figure 11**, are interpolations performed for input values, and those obtained through theoretical analysis. Interpolations are used as auxiliary tools to obtain fundamental quantities related to the thermal

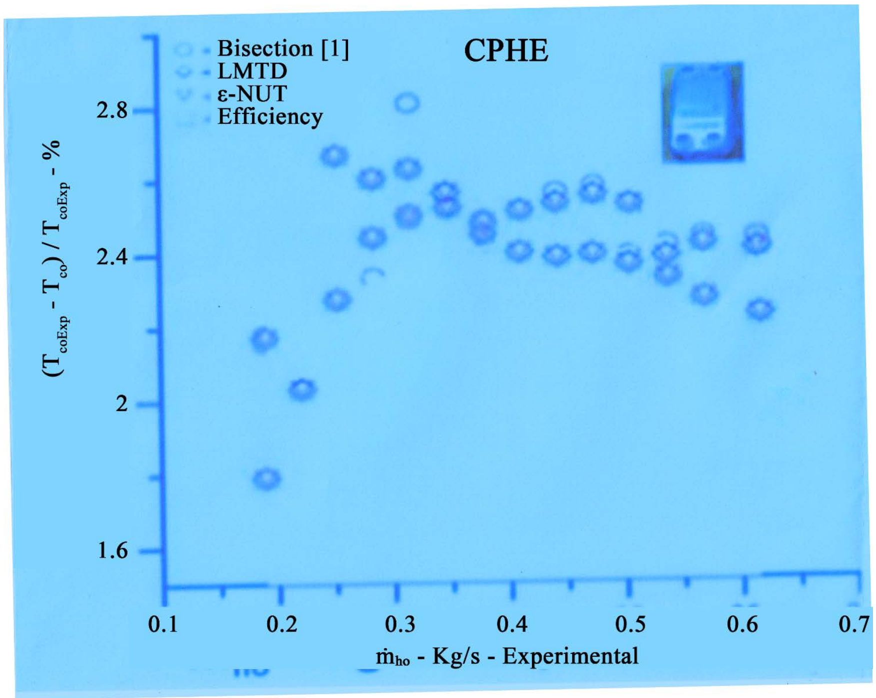

Figure 10. Percentage error for cold fluid outlet temperature T_{co}.

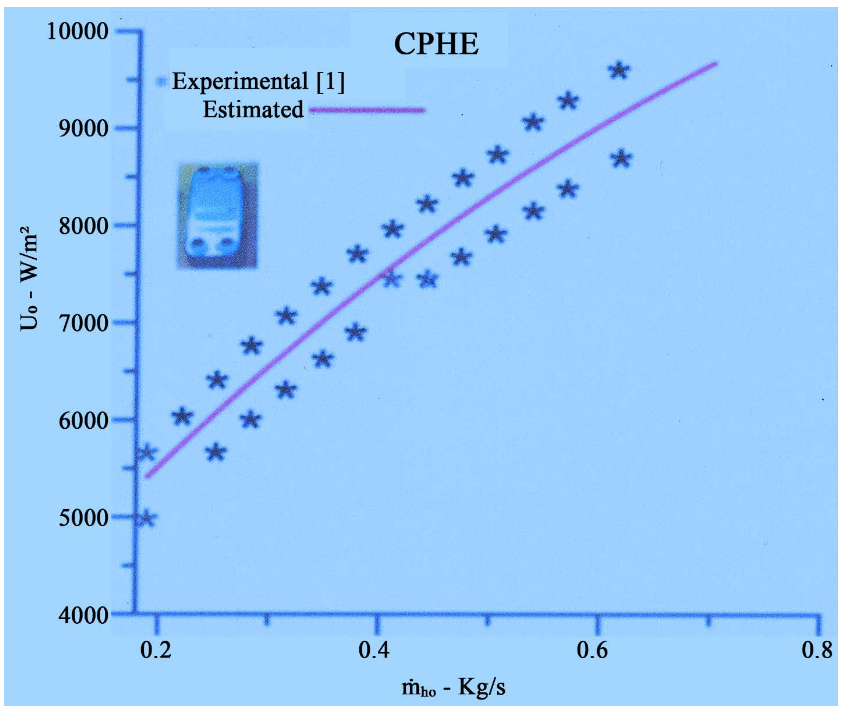

Figure 11. Overall heat transfer coefficient versus mass flow rate of the hot fluid.

performance of the heat exchanger.

Figure 12 and Figure 13 show two sets of values obtained for the outlet temperature of the hot fluid and cold fluid using efficiency methods, in comparison to experimental data.

Theoretical results obtained for thermal efficiency (Figure 14) and heat transfer rate (Figure 15) for CPHE-1 are shown above.

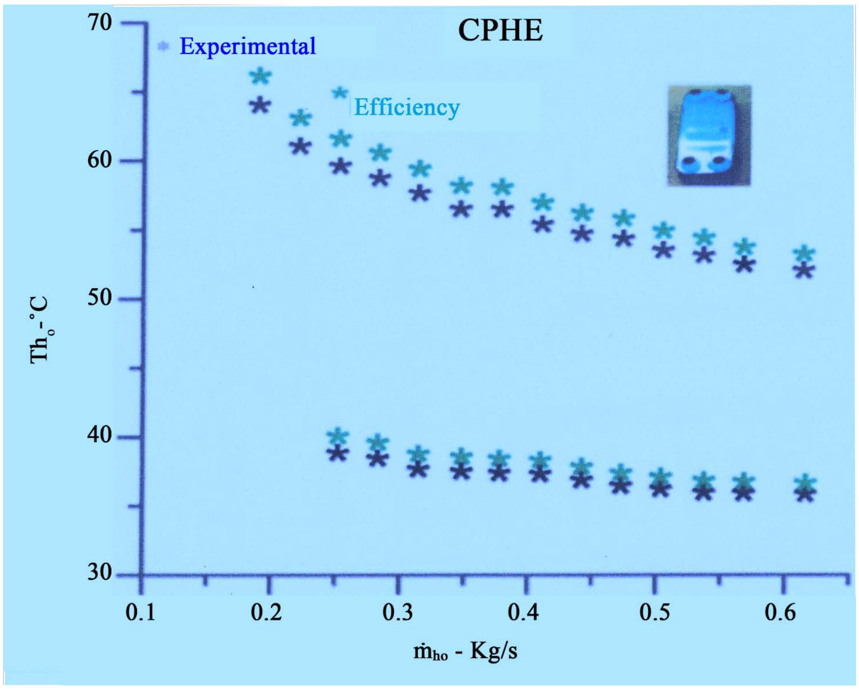

Figure 12. Hot fluid outlet temperature versus hot fluid mass flow rate.

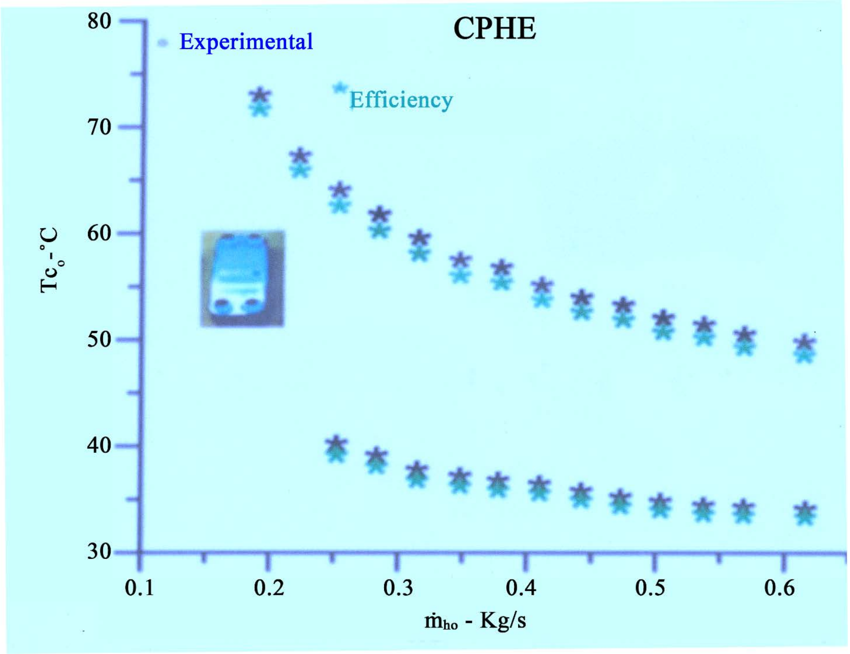

Figure 13. Outlet temperature of cold fluid versus mass flow rate of hot fluid.

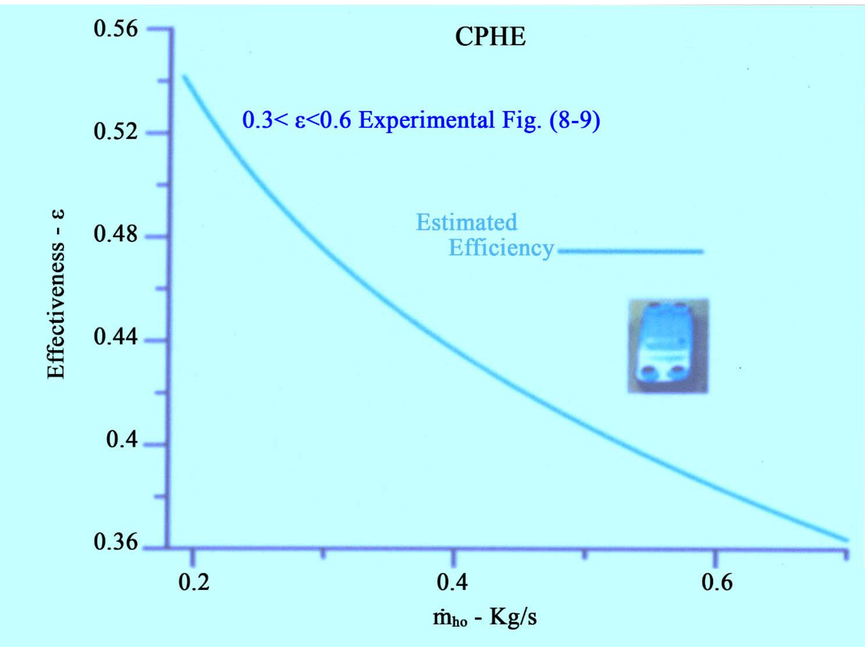

Figure 14. Thermal effectiveness versus mass flow rate of hot fluid.

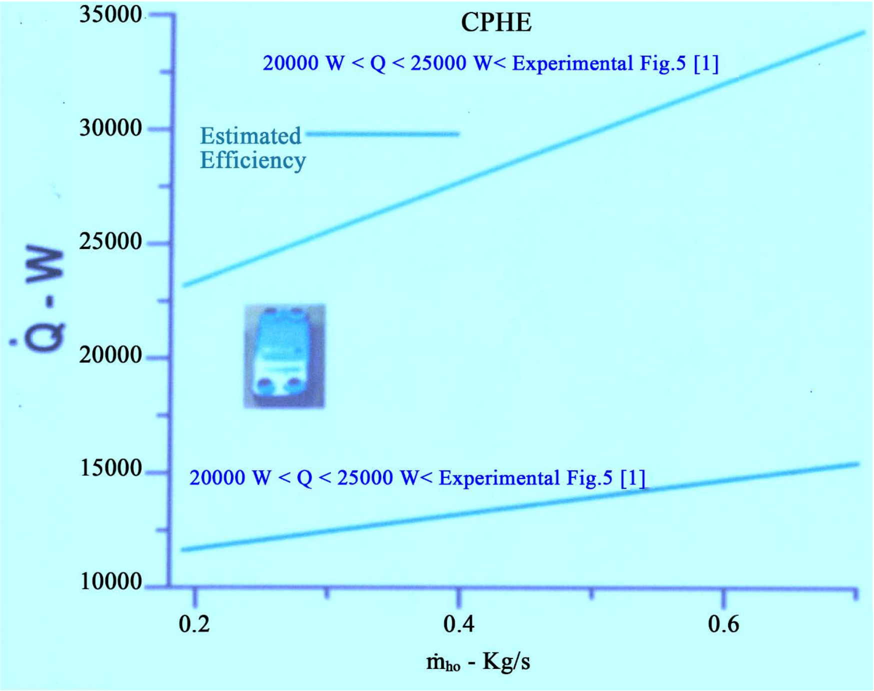

Figure 15. Heat transfer rate versus mass flow rate of the hot fluid.

The theoretical results presented in Figure 14 for thermal effectiveness show values consistent with similar graphical results to those presented in the reference work (Figure 8 and Figure 9), across the entire flow rate range analyzed. The thermal efficiency is not very high and decreases with flow rate, as expected for compact heat exchangers, where viscous dissipation is high and significantly affects thermal performance.

Figure 15 presents theoretical results for the heat transfer rate. The theoretical analysis was performed on the two ranges of input values, as previously highlighted for other physical quantities. The theoretical results obtained demonstrate numerical consistency with respect to the results presented in **Figure 15** [1] of the reference work.

The estimated values for the heat transfer rate and thermal efficiency were obtained using the thermal efficiency method and experimental quantities obtained from the reference work (Figure 20 [1] and Figure 20.1 [1]), including mass flow rates, inlet and outlet temperatures of the hot and cold fluids.

4. Analysis Performed for Other Heat Exchangers Evaluated through the Reference Work [1]

4.1. Heat Exchangers with Different Physical Specifications Were Also Analyzed by the Authors of the Reference Work [1]

The heat exchangers are theoretically analyzed and named CPHE-2, CPHE-3, and CPHE-4.

Physical and geometric parameters used, analyzed, and compared through the methods mentioned in this article were obtained from (CPH-2), (CPH-3) and (CPH-4) from the reference work. Gaps observed through the data available in these tables are the heat exchanger areas.

Estimated average areas for heat exchangers CPHE-2, CPHE-3, and CPHE-4 were obtained from available experimental data and are shown in **Figure 16**. The values used to determine the average areas were obtained using the following expression:

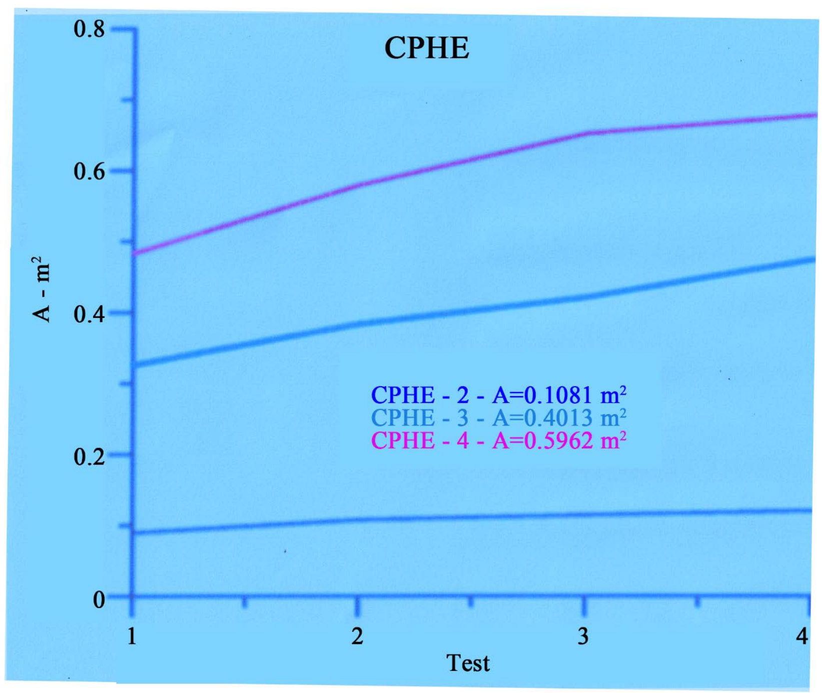

Figure 16. CPHEs real areas.

$$A_{tranf} = \left(\dot{m}_c C_{pc} * \left(Tco_{Exp} - Tci_{Exp}\right)\right) / \left(U_O * \Delta T_{lm}\right) \quad (25)$$

The real areas, for CPHE-2, CPHE-3, and CPHE-4 are highlighted in Figure 16.

Results obtained using the most probable areas are represented in items 4.2.2, 4.3.2, and 4.4.2, associated with items 4.2—CPH2, 4.3—CPH3, and 4.4—CPH4, below.

The analysis performed for each of the heat exchangers is conducted in two stages:

1) Areas of the heat exchangers equal to the area of the reference heat exchanger (CPH-1), equal to ($A_{Transf} = 0.168\ \text{m}^2$), with the objective of analysis, comparison of theoretical-experimental results, and discussion;

2) Actual areas of the heat exchangers, obtained through Equation (23), for effective determination of the theoretical outlet temperatures, comparison with experimental results and discussion regarding the results obtained through stage 1.

4.2. Analysis and Discussion of the Theoretical Results Obtained for CPHE-2

The CPHE-2 heat exchanger, with the dimensions stipulated through the reference work, is represented in Figure 17.

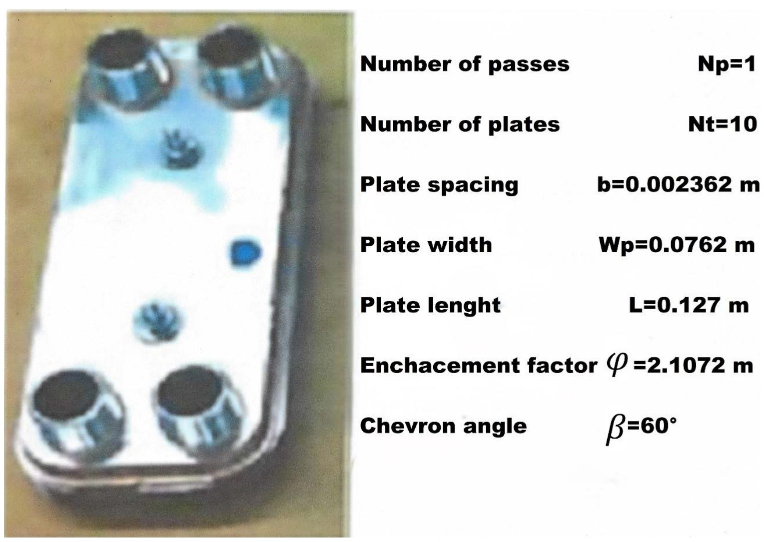

Figure 17. Chevron Plate Heat Exchanger—CPHE-2 [1].

4.2.1. Results for CPHE-2 Using the Media Area of CPH-1

Table 1 and Table 2 present theoretical and experimental results associated with the CPHE-2 plate heat exchanger, using, for comparison and discussion, the same area of CPHE-1.

Table 1 presents experimental values obtained for inlet and outlet temperatures of the cold and hot fluids (columns 1-4). Columns 5 and 6 present values obtained through the bisection method, and columns 7 and 8 present values obtained through the application of the thermal efficiency method.

Table 1. Theoretical and experimental data obtained for the CPHE-2 heat exchanger using area of CPHE-1.

$\dot{m}_h$ Kg/s	T_{hi} ˚C Exp	T_{ci} ˚C Exp	T_{ho} ˚C Exp	T_{co} ˚C Exp	T_{ho} ˚C Bisec	T_{co} ˚C Bisec	T_{ho} ˚C Effic	T_{co} ˚C Effic
0.189504	54.74	24.43	41.11	37.62	40.89	38.29	42.43	36.74
0.347256	45.07	25.22	37.56	32.63	38.12	32.16	35.48	34.80
0.441504	41.57	24.56	35.61	30.47	36.31	29.83	34.14	32.01
0.472311	67.94	37.58	56.90	48.52	58.48	47.06	54.58	50.96

Table 2 presents percentage errors obtained for the bisection method [1] and the thermal efficiency method. The percentage errors obtained using the bisection method are between 0.53% and 3.00%. The percentage errors obtained using the thermal efficiency method are between 3.21% and 6.65%. It can be observed that the errors increase with increasing mass flow rate.

Table 2. Percentage errors obtained by the bisection method [1] and the efficiency method for CPHE-2 using area of CPHE-1.

$\dot{m}_h$ Kg/s	T_{ho} ˚C Bisec %	T_{co} ˚C Bisec %	T_{ho} ˚C Effic %	T_{co} ˚C Effic %
0.189504	0.53	1.78	3.21	2.34
0.347256	1.45	1.44	5.55	6.65
0.441504	1.96	2.10	4.13	5.05
0.472311	2.78	3.00	4.08	5.03

The differences observed in the errors in Table 2 should be attributed to the difference in heat exchange area between the CPHE-1 and CPHE-2 heat exchangers, and not to the methods analyzed. However, the deviations, in this case, are not significantly high, as the medium areas between the heat exchangers are very close.

The deviations observed for the thermal efficiency method are slightly larger than those observed for the bisection method, as expected in this case.

4.2.2. Results for CPHE-2 Using the Real Area

Table 3 presents theoretical results obtained through the application of thermal effectiveness (ε-NTU) and thermal efficiency methods. As expected, the results obtained for the fluid outlet temperatures are remarkably close to the experimental values and cannot observed difference between the absolute theoretical values.

Table 4 presents the deviation results obtained through the application of the thermal effectiveness method, for the two conditions analyzed: area equal to CPHE-1 and actual area for CPHE-2. As expected, When the areas are the effective areas for CPHE-2, the deviations are significantly smaller, below 1.0%.

Results obtained for thermal effectiveness are presented in Table 5 for comparisons between two stages. The results obtained reflect the differences related to the areas under analysis: higher values for larger heat exchange areas.

Table 3. Theoretical and experimental data obtained for the CPHE-2 heat exchanger real area.

$\dot{m}_h$ Kg/s	T_{hi} ˚C Exp	T_{ci} ˚C Exp	T_{ho} ˚C Exp	T_{co} ˚C Exp	T_{ho} ˚C ε-NTU	T_{co} ˚C ε-NTU	T_{ho} ˚C Effic	T_{co} ˚C Effic
0.189504	54.74	24.43	41.11	37.62	41.45	37.72	41.45	37.72
0.347256	45.07	25.22	37.56	32.63	37.65	32.64	37.65	32.64
0.441504	41.57	24.56	35.61	30.47	35.68	30.45	35.68	30.45
0.472311	67.94	37.58	56.90	48.52	56.97	48.55	56.97	48.55

Table 4. Percentage of errors obtained using the efficiency method for the two stages for CPHE-2.

$\dot{m}_h$ Kg/s	T_{ho} ˚C Effic %	T_{co} ˚C Effic %	T_{ho} ˚C Effic %	T_{co} ˚C Effic %
0.189504	3.21	2.34	0.83	0.27
0.347256	5.55	6.65	0.24	0.03
0.441504	4.13	5.05	0.20	0.06
0.472311	4.08	5.03	0.12	0.06

Table 5. Comparison between effectiveness for two stage for CPHE-2.

$\dot{m}_h$ Kg/s	ε	Area m^2	ε	Real area m^2
0.189504	0.594	0.168	0.438	0.0897
0.347256	0.482	0.168	0.376	0.1076
0.441504	0.438	0.168	0.346	0.1143
0.472311	0.441	0.168	0.361	0.1206

It should be noted, in this case, that real thermal effectiveness is significantly low, reflecting the small configuration of the heat exchanger and possible high viscous dissipation.

4.3. Analysis and Discussion of the Theoretical Results Obtained for CPHE-3

The CPHE-3 heat exchanger, with the dimensions stipulated through Table 4 in the work of reference, is represented in Figure 18.

4.3.1. Results for CPHE-3 Using the Media Area of CPH-1

Table 6 and Table 7 present theoretical and experimental results associated with the CPHE-3 plate heat exchanger.

Table 6 presents experimental values obtained for inlet and outlet temperatures of the cold and hot fluids (columns 1-4). Columns 5 and 6 present values obtained through the bisection method, and columns 7 and 8 present values obtained through the application of the thermal efficiency method for CPHE-3.

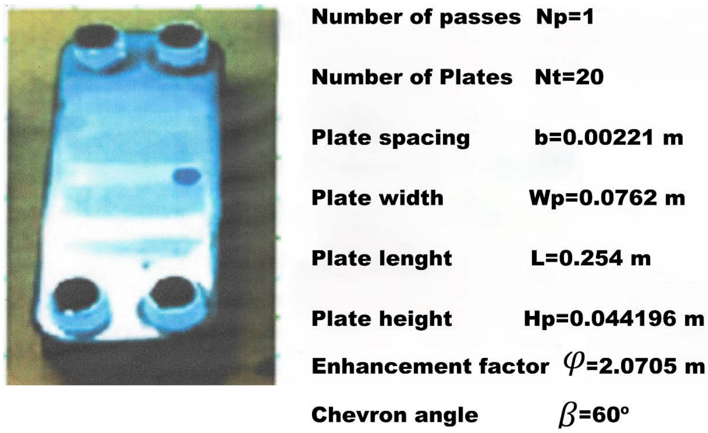

Figure 18. Chevron Plate Heat Exchanger—CPHE-3 [1].

Table 6. Theoretical and experimental data obtained for the CPHE-3 heat exchanger using the area of CPHE-1.

$\dot{m}_h$ Kg/s	T_{hi} ˚C	T_{ci} ˚C	T_{ho} ˚C Exp	T_{co} ˚C Exp	T_{ho} ˚C Bisec	T_{co} ˚C Bisec	T_{ho} ˚C Effic	T_{co} ˚C Effic
0.190323	51.07	26.42	33.60	44.31	33.11	44.39	33.22	42.28
0.346374	43.47	28.16	33.56	37.88	33.63	37.95	36.77	34.82
0.506394	37.71	26.65	31.02	33.26	31.34	33.02	33.60	30.76
0.693315	58.24	41.88	48.69	51.41	49.52	50.59	52.82	47.29

Table 7 presents percentage errors obtained for the bisection method and the thermal efficiency method. The percentage errors obtained using the bisection method are between 0.20% and 1.70%. The percentage errors obtained using the thermal efficiency method are between 1.10% and 9.60%. It can be observed that the errors increase with increasing mass flow rate.

Table 7. Percentage errors obtained by the bisection method [1] and the efficiency method using area of CPHE-1.

$\dot{m}_h$ Kg/s	T_{ho} ˚C Bisec %	T_{co} ˚C Bisec %	T_{ho} ˚C Effic %	T_{co} ˚C Effic %
0.190323	1.46	0.20	1.10	4.60
0.346374	0.20	0.20	9.60	8.10
0.506394	1.03	0.72	8.32	7.52
0.693315	1.70	1.60	8.50	8.01

The differences observed in the errors in Table 7 should be attributed to the difference in heat exchange area between the CPHE-1 and CPHE-3 heat exchangers, and not to the methods analyzed. However, the deviations, in this case, are relatively high, since the areas between the heat exchangers are significantly different. The deviations observed for the thermal efficiency method are greater than those observed for the bisection method, as expected in this case.

4.3.2. Results for CPHE-3 Using the Real Area

Table 8 presents theoretical results obtained through the application of thermal effectiveness and thermal efficiency methods. As expected, the results obtained for the fluid outlet temperatures are very close to the experimental values, with equal values for both methods analyzed.

Table 9 presents the deviation results obtained through the application of the thermal effectiveness method, for the two conditions analyzed: area equal to CPHE-1 and actual area for CPHE-3. When the areas are the effective areas for CPHE-3, the deviations are significantly smaller, below 2.0%.

Results obtained for thermal effectiveness are presented in Table 10, for comparisons between two stages. The results obtained reflect the differences related to the areas under analysis: higher values for larger heat exchange areas.

Table 8. Theoretical and experimental data obtained for the CPHE-3 heat exchanger real area.

$\dot{m}_h$ Kg/s	T_{hi} ˚C	T_{ci} ˚C	T_{ho} ˚C Exp	T_{co} ˚C Exp	T_{ho} ˚C ε-NTU	T_{co} ˚C ε-NTU	T_{ho} ˚C Effic	T_{co} ˚C Effic
0.190323	51.07	26.42	33.60	44.31	33.97	43.52	33.97	43.52
0.346374	43.47	28.16	33.56	37.88	33.71	37.91	33.71	37.91
0.506394	37.71	26.65	31.02	33.26	30.77	33.15	30.77	33.15
0.693315	58.24	41.88	48.69	51.41	48.71	51.41	48.71	51.41

Table 9. Percentage of error obtained using the efficiency method for the two stages for CPHE-3.

$\dot{m}_h$ Kg/s	T_{ho} ˚C Effic %	T_{co} ˚C Effic %	T_{ho} ˚C Effic %	T_{co} ˚C Effic %
0.190323	1.10	4.60	1.01	1.78
0.346374	9.60	8.10	0.45	0.07
0.506394	8.32	7.52	0.81	0.33
0.693315	8.50	8.01	0.41	0.00

Table 10. Comparison between effectiveness for two stages for CPHE-3.

$\dot{m}_h$ Kg/s	ε	Area m^2	ε	Real area m^2
0.190323	0.538	0.168	0.694	0.3265
0.346374	0.436	0.168	0.638	0.3842
0.506394	0.371	0.168	0.600	0.4267
0.693315	0.3308	0.168	0.582	0.4742

In this case, it should be noted that the actual thermal effectiveness is still low, reflecting the relatively average configuration of the heat exchanger and the possible moderate viscous dissipation.

4.4. Analysis and Discussion of the Theoretical Results Obtained for CPHE-4

The CPHE-4 heat exchanger, with the dimensions stipulated through Table 6 in the work of reference, is represented in Figure 19.

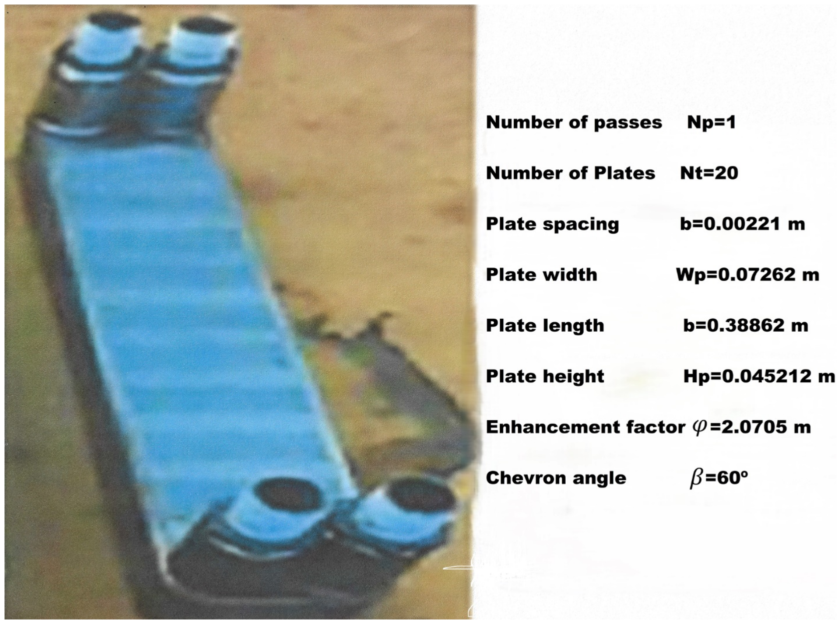

Figure 19. Chevron plate heat exchanger—CPHE-4 [1].

4.4.1. Results for CPHE-4 Using the Media Area of CPH-4

Table 11 and Table 12 present theoretical and experimental results associated with the CPHE-4 plate heat exchanger.

Table 11 presents experimental values obtained for inlet and outlet temperatures of the cold and hot fluids (columns 1-4). Columns 5 and 6 present values obtained through the bisection method, and columns 7 and 8 present values obtained through the application of the thermal efficiency method for CPHE-4.

Table 11. Theoretical and experimental data obtained for the CPHE-4 heat using area of CPHE-1.

$\dot{m}_h$ Kg/s	T_{hi} ˚C	T_{ci} ˚C	T_{ho} ˚C Exp	T_{co} ˚C Exp	T_{ho} ˚C Bisec	T_{co} ˚C Bisec	T_{ho} ˚C Effic	T_{co} ˚C Effic
0.190134	51.24	29.53	34.22	46.06	33.80	47.01	39.57	41.22
0.378567	42.26	30.34	33.65	38.82	33.68	38.92	37.24	35.37
0.567252	39.18	30.73	33.41	36.46	33.62	36.30	36.19	33.72
0.630819	59.35	44.52	49.21	54.62	48.68	54.19	54.21	49.67

Table 11 presents percentage errors obtained for the bisection method and the thermal efficiency method. The percentage errors obtained using the bisection method range from 0.00% to 8.90%. The percentage errors obtained using the thermal efficiency method range from 7.51% to 15.63%.

Table 12. Percentage errors obtained by the bisection method and the efficiency method for CPHE-4.

$\dot{m}_h$ Kg/s	T_{ho} ˚C Bisec %	T_{co} ˚C Bisec %	T_{ho} ˚C Effic %	T_{co} ˚C Effic %
0.190134	1.22	2.06	15.63	10.51
0.378567	0.00	8.9	10.67	8.89
0.567252	0.62	0.44	8.32	7.51
0.630819	0.85	0.78	10.16	9.06

The differences observed in the errors in Table 11 should be attributed to the difference in heat exchange area between the CPHE-1 and CPHE-4 heat exchangers, and not to the methods analyzed.

However, the deviations, in this case, are relatively high, since the areas between the heat exchangers are significantly different. The deviations observed for the thermal efficiency method are greater than those observed for the bisection method, as expected in this case.

4.4.2. Results for CPHE-4 Using the Real Area

Table 13 presents theoretical results obtained through the application of thermal effectiveness and thermal efficiency methods. As expected, the results obtained for the fluid outlet temperatures are very close to the experimental values, with equal values for both methods analyzed.

Table 13. Theoretical and experimental data obtained for the CPHE-4 heat exchanger real area.

$\dot{m}_h$ Kg/s	T_{hi} ˚C	T_{ci} ˚C	T_{ho} ˚C Exp	T_{co} ˚C Exp	T_{ho} ˚C ε-NTU	T_{co} ˚C ε-NTU	T_{ho} ˚C Effic	T_{co} ˚C Effic
0.190134	51.24	29.53	34.22	46.06	34.50	46.27	34.50	46.27
0.378567	42.26	30.34	33.65	38.82	33.73	38.87	33.73	38.87
0.567252	39.18	30.73	33.41	36.46	33.44	36.47	33.44	36.47
0.630819	59.35	44.52	49.21	54.62	49.23	54.64	49.23	54.64

Table 14 presents the deviation results obtained through the application of the thermal efficiency method, for the two conditions analyzed: area equal to CPHE-1 and actual area for CPHE-4. When the areas are the effective areas for CPHE-3, the deviations are significantly smaller, below 1.0%.

Results obtained for thermal effectiveness are presented in Table 15, for comparisons between two stages. The results obtained reflect the differences related to the areas under analysis: higher values for larger heat exchange areas.

Table 14. CPHE-4 percentage of errors obtained using the efficiency method for the two stages.

$\dot{m}_h$ Kg/s	T_{ho} ˚C Effic %	T_{co} ˚C Effic %	T_{ho} ˚C Effic %	T_{co} ˚C Effic %
0.190134	15.63	10.51	0.81	0.46
0.378567	10.67	8.89	0.24	0.03
0.567252	8.32	7.51	0.09	0.03
0.630819	10.16	9.06	0.04	0.04

Table 15. CPHE-4 comparison between effectiveness for two stages, for different areas.

$\dot{m}_h$ Kg/s	Area m^2	ε	ε	Real area m^2
0.190134	0.168	0.539	0.771	0.4834
0.378567	0.168	0.422	0.638	0.3842
0.567252	0.168	0.354	0.680	0.6519
0.630819	0.168	0.347	0.682	0.6780

In Table 15 it should be noted that the actual thermal effectiveness is relatively high, reflecting the relatively high configuration of the heat exchanger and the possible low viscous dissipation.

4.5. Final Considerations about the Results Presented for CPHEs

1) The differences observed between the errors obtained for attributed areas equal to the CPHE-1 are a possible difference in heat exchange area between the CPHE-1 and others CPHE heat exchangers, and not due to the methods analyzed;

2) Thermal effectiveness are higher when the dimensions of the heat exchangers increase;

3) Thermal efficiencies are very close to unity, due to the values of the thermal capacities associated with the fluids, which in all cases analyzed are very close to each other;

4) Analysis of thermal and viscous irreversibilities, through the Bejan number, if performed, allows for study related to the cost-benefit associated with the heat exchangers.

5. Conclusions

This study and comparative analysis utilizes four theoretical methods to solve heat exchange problems associated with four heat exchangers. It presents a practical and low-cost procedure for the preliminary prediction of the thermal performance of chevron plate heat exchangers (CPHEs), also pointing to broader design and research topics—such as the relationship between pressure drop and heat transfer, geometric optimization, irreversibility, and advanced working fluids—that can be explored beyond the base case.

It can be concluded that the methods used are compatible and present very similar values related to heat exchange for CPHE-1. However, when the areas assigned to the other three heat exchangers are made equal to the media area of CPH-1, for analysis and discussion, the errors become significantly more pronounced. These latter results can be attributed to the larger area of the other heat exchangers. The deviations between theoretical and experimental values, in these cases, range from 1.1% to 15.6%.

When actual heat exchanger areas are correctly assigned to the others heat exchangers, the errors between the effectiveness (ε-NTU) method and the thermal efficiency method, when compared with experimental values, range from 0.00% to 1.01%, demonstrating the consistency of the two theoretical procedures.

It is worth noting that the study carried out can be used as a teaching tool to be replicated in courses on heat exchangers. As an additional exercise, in this case, an analysis related to the relationship between thermal and viscous irreversibilities, represented by the Bejan number, can be useful to determine the cost-benefit relationships associated with the thermally analyzed heat exchangers.

Author Contributions

Élcio Nogueira: Analytical Modeling, Introduction and Discussion. João Vitor Santana: Computational Modeling and Conclusion. The authors declare no conflict of interest regarding publication of this paper.

Conflicts of Interest

The authors declare no conflicts of interest regarding the publication of this paper.

References

[1] Bhattad, A., Atgur, V., Rao, B.N., Banapurmath, N.R., Manavendra, G., Sajjan, A.M., *et al*. (2024) A Simplified LMTD Approach to Assess the Effectiveness of a Chevron-Type Plate Heat Exchanger. *Journal of Thermal Analysis and Calorimetry*, **149**, 12205-12217. https://doi.org/10.1007/s10973-024-13573-y

[2] Nogueira, É. (2025) Heat Exchangers: Analytical Modeling and Applications. Editora Dialética.

[3] Zhao, Y., Liu, H.Y., Zhang, L. and Wang, C.C. (2024) Effect of Chevron Angle on the Thermofluids Performance of Shell-and-Plate Heat Exchangers—A Numerical Approach. *Applied Thermal Engineering*, **239**, Article 122061. https://doi.org/10.1016/j.applthermaleng.2023.122061

[4] Adarsh Varma, P., SatyaPriya, C., Prashanth, M., Mukesh, P., Sai Sri Nandan, B., Srinivas, G., *et al*. (2024) Nanofluids for Heat Transfer Augmentation in Heat Exchangers—An Overview of Current Research. In: *Lecture Notes in Mechanical Engineering*, Springer, 83-95. https://doi.org/10.1007/978-981-99-5990-7_8

[5] Arsenyeva, O., Tovazhnyanskyy, L., Kapustenko, P., Klemeš, J.J. and Varbanov, P.S.

(2023) Review of Developments in Plate Heat Exchanger Heat Transfer Enhancement for Single-Phase Applications in Process Industries. *Energies*, **16**, Article 4976. https://doi.org/10.3390/en16134976

[6] Zhang, J., Zhou, N., Zhang, G. and Tian, M. (2023) Numerical and Experimental Studies of Flow and Heat Transfer Characteristics in a Plate Heat Exchanger with Multi-Chevron Corrugate Furrows. *Numerical Heat Transfer*, *Part A*: *Applications*, **84**, 71-82. https://doi.org/10.1080/10407782.2022.2105076

[7] Ham, J., Lee, G., Kwon, O., Bae, K. and Cho, H. (2023) Numerical Study on the Flow Maldistribution Characteristics of a Plate Heat Exchanger. *Applied Thermal Engineering*, **224**, Article 120136. https://doi.org/10.1016/j.applthermaleng.2023.120136

[8] Sohn, S., Kim, J., Yoo, J.W., Chung, Y., Lee, K.H. and Song, C.H. (2023) Effect of Flow Path on the Performance of Plate Heat Exchanger with Chevron Shape. *Journal of Mechanical Science and Technology*, **37**, 1523-1530. https://doi.org/10.1007/s12206-023-0237-8

[9] García-Castillo, J.L., Crespo-Quintanilla, J.A. and Picón-Núñez, M. (2024) A Novel Design Approach of Plate Heat Exchangers Considering the Economic Impact of Chevron Angles. *Chemical Engineering and Processing—Process Intensification*, **199**, Article 109759. https://doi.org/10.1016/j.cep.2024.109759

[10] Sadeghianjahromi, A., Jafari, A. and Wang, C.C. (2022) Numerical Investigation of the Effect of Chevron Angle on Thermofluids Characteristics of Non-Mixed and Mixed Brazed Plate Heat Exchangers with Experimental Validation. *International Journal of Heat and Mass Transfer*, **184**, Article 122278. https://doi.org/10.1016/j.ijheatmasstransfer.2021.122278

[11] Nogueira, É. (2022) Theoretical Analysis of the Influence of the Chevron Inclination Angle on the Thermal Performance of a Gasket Plate Heat Exchanger. *Acta Polytechnica*, **62**, 627-638. https://doi.org/10.14311/ap.2022.62.0627

[12] Nogueira, É. (2022) Entropy Generation Analysis in a Gasket Plate Heat Exchanger Using Non-Spherical Shape of Alumina Boehmite Nanoparticles. *Ovidius University Annals of Chemistry*, **33**, 41-49. https://doi.org/10.2478/auoc-2022-0006

[13] Rezende, T.R., Vianna, R.F. and Luporini, S. (2021) Simulation of a Plate Heat Exchanger Operating with Nanofluid Coolant Using CFD. *International Journal of Heat and Technology*, **39**, 235-240. https://doi.org/10.18280/ijht.390126

[14] Gupta, S.K., Gupta, S., Gupta, T., Raghav, A. and Singh, A. (2021) A Review on Recent Advances and Applications of Nanofluids in Plate Heat Exchanger. *Materials Today*: *Proceedings*, **44**, 229-241. https://doi.org/10.1016/j.matpr.2020.09.460

[15] Dutta, O.Y. and Rao, B.N. (2018) Investigations on the Performance of Chevron Type Plate Heat Exchangers. *Heat and Mass Transfer*, **54**, 227-239. https://doi.org/10.1007/s00231-017-2107-3

[16] Nogueira, É. (2018) Theoretical Analysis of Heat Transfer in a Gasket Chevron Corrugated Plate Heat Exchanger Used for Vegetable Oils Refrigeration. *The International Journal of Engineering and Science*, **7**, 56-59.

[17] Fakheri, A. (2007) Heat Exchanger Efficiency. *Journal of Heat Transfer*, **129**, 1268-1276. https://doi.org/10.1115/1.2739620

Nomenclature

A_{trans}	heat transfer area, [m^2]
C_p	specific heat, [J/kg K]
C	thermal capacity, [W/K]
C_{min}	minimum thermal capacity, [W/K]
$C^* = C_{min}/C_{max}$	
Fa	fin analogy
K	Kelvin
$\dot{m}_c$	mass flow rate of the air, [kg/s]
$\dot{Q}$	heat transfer rate, [W]
T	temperatures, [˚C]
U_o	global heat transfer coefficient, [W/(m^2 K)]

Greek Symbols

ε_T	thermal effectiveness
η_T	thermal efficiency
ΔT	a difference of temperatures, [˚C]